Experimental Pancreatic Carcinogenesis

I. Morphogenesis of Pancreatic Adenocarcinoma in the Syrian Golden Hamster Induced by N-Nitroso-bis(2-hydroxypropyl)amine

Morton H. Levitt, MD, Curtis C. Harris, MD, Robert Squire, DVM, PhD, Stephen Springer, MS, Martin Wenk, PhD, Cynthia Mollelo, Delma Thomas, HT (ASCP), Elizabeth Kingsbury, PhD, and Carnell Newkirk, BS

In a serial sacrifice experiment, outbred male Syrian golden hamsters were treated once weekly for life with subcutaneous injections of *N*-nitroso-bis(2-hydroxypropyl)amine (DIPN). The pancreas was examined by high resolution light (1-μ sections) and transmission electron microscopy. Early nonspecific changes in all pancreatic epithelial cellular elements were followed by a progressive proliferation of intra- and interlobular duct cells, with the development of multicentric foci of cystic and papillary cystic adenomas, intraductal carcinomas, and invasive ductal neoplasms. These observations were consistent with a multistage morphogenesis of pancreatic adenocarcinoma of ductal origin. (Am J Pathol 88:5–28, 1977)

CANCER OF THE PANCREAS now ranks fourth as a cause of cancer deaths,[1] estimated [2] to have accounted for more than 19,000 deaths in 1976 and 22,000 new cases. If the present rate continues, the incidence in the index year 1969 may double by the end of the century.[3]

Until recently, no practical experimental model for the induction and study of cancer of the pancreas has been available. However, in 1974 a new and significant model for experimental pancreatic carcinogenesis was described.[4]

In the present report, we described the appearance by high resolution light (1-μ sections) and transmission electron microscopy of induced pancreatic neoplasms in the Syrian golden hamster following subcutaneous injections of *N*-nitroso-bis(2-hydroxypropyl)amine (synonyms: 2,2′-dihydroxy-di-*N*-propylnitrosamine, diisopropanolnitrosamine; DIPN, DHPN and BHP).

From the Experimental Pathology Branch, Carcinogenesis Program, Division of Cancer Cause and Prevention, National Cancer Institute, Bethesda, Maryland; and Microbiological Associates, Bethesda, Maryland; and Litton-Bionetics, Inc., Kensington, Maryland.

Supported in part by Contracts N01-CP-02199 and NO1-CP-22063 from the National Cancer Institute.

Presented in part at the Sixty-fifth Annual Meeting of the International Academy of Pathology (US-Canadian Division), Boston, Mass., March 23, 1976.

Accepted for publication March 22, 1977.

Address reprint requests to Dr. Morton H. Levitt, Building 37, Room 3A19, National Cancer Institute, National Institutes of Health, Bethesda, MD 20014.

Materials and Methods

Animals

One hundred and thirty outbred 6-week-old male Syrian golden hamsters (A. R. Schmidt Co., Madison, Wisc.) were used. They were held for 2 weeks, housed in polycarbonate cages in groups of 4 on Bed-O-Cobs bedding (Anderson Cob Mills, Inc., Maumee, Ohio), fed Purina Lab Chow and water *ad libitum*, and kept under standardized conditions (temperature, 21 ± 3 C; humidity, 40 ± 5%; 10 air changes/hr; light/dark cycle, 12 hrs/12 hrs).

Experimental Design

In one experiment, 52 hamsters received a weekly subcutaneous injection of DIPN (250 mg/kg body weight) suspended in olive oil. Thirteen control hamsters received an equivalent volume of olive oil. One hour prior to sacrifice, 4 test and 1 control hamster received an intraperitoneal injection of ^{3}H-thymidine (specific activity, 6.7 Ci/mM; concentration, 3 μCi/g body weight). The animals were serially sacrificed at 1 hour and 1, 2, 5, 10, 12, 15, 17, 20, 22, 26, 30, and 31 weeks.

In a second parallel experiment, deionized water was substituted for olive oil as the vehicle for the carcinogen. Since animal survival was shortened, the final two sacrifices were performed at 23 and 26 weeks.

Carcinogen

The DIPN (Ash-Stevens Inc., Detroit, Mich.) has an analysis as follows: λ max 236 mμ (ϵ 7,220); TLC-homogenous in ether methanol (11 : 1) on Brinkman Polygram Sil G/UV$_{254}$ *Rf* = 0.46. The DIPN was stored at 4 C in the dark and warmed to room temperature before use.

Tissues, Fixation, and Embedding

After halothane anesthesia, the abdominal cavity was opened, the pancreas removed immediately, diced into 1- to 2-mm cubes, and fixed overnight at 4 C in 2.7% glutaraldehyde (EM grade), buffered to pH 7.4 with 0.2 M *s*-collidine. The tissues were then postfixed for 2 hours in similarly buffered 1.3% osmium tetroxide.

Following serial dehydration, the tissues were embedded in Epon 812 containing 5% Araldite, vacuumed to remove air bubbles, and cured for 72 hours at 60 C.

Microscopy

One-micron sections were prepared on an LKB ultramicrotome, stained for 1 hour at 24 C with toluidine blue, and coverslipped using Eastman 910 compound. Selected sections were cut at 800 to 900 Å, and stained with uranyl acetate and lead citrate for 60 and 5 minutes, respectively.

Ultrathin sections were examined on a Siemens 1A or Hitachi HU 12A transmission electron microscope.

Autoradiography

The ^{3}H-thymidine was obtained from New England Nuclear Corp., Boston, Mass. The 1-μ sections (see above) were exposed and developed according to previously published procedures.[5]

In evaluating the autoradiograms, 1000 acinar, 300 duct, and 300 islet cells were counted under oil immersion (1000 ×) in a systematic fashion until the total number of cells was

reached. Proliferative lesions as well as normal cells were counted. A cell was considered labeled if it possessed four or more grains over the nucleus.

Morphologic criteria to identify acinar, duct, and islet cells in 1-μ toluidine blue–stained sections were established before counting began. Normal cells were readily distinguished on the basis of their nuclear and cytoplasmic features. However, dilated degranulated acini often resembled pancreatic ducts. We considered cells from the former to be those which were relatively hyperchromatic, with coarse chromatin and very prominent, usually multiple, centrally placed nucleoli.

Results

Autoradiography

The results are shown in Tables 1-6. Labeling indices for acinar, duct and islet cells are tabulated for the DIPN in olive oil experiments (Tables 1, 3, and 5) and for the DIPN in H_2O experiments (Tables 2, 4, and 6).

Comparison of the results from the two experiments indicated that significant ($P < 0.05$) increases in the ^{3}H-TdR labeling indices in pancreatic acinar and duct cells over those for control animals were noted at 22 experimental weeks (olive oil vehicle) and at 10 weeks (H_2O vehicle). In neither experiment was there a significant difference between experimental and control groups for pancreatic islet cells.

Since the data manifested large standard deviations, we also analyzed the results using a nonparametric randomization test.[6] This procedure requires no assumptions of statistical normality or equality of variances in the groups involved (which are assumed if the equivalent parametric test, the t test, is used). The results shown in Tables 1–6 were substantiated upon application of this procedure, indicating that despite the large standard deviations the results were valid.

Light and Electron Microscopy

The induced pancreatic lesions went through a reproducible morphologic pattern as a function of time, although the progression to carcinoma was accelerated in the second experiment (DIPN in H_2O).

In comparison to normal cells (Figures 1–3),[7,8] ultrastructural changes in pancreatic duct and acinar cells (Figures 4 and 5) could be readily appreciated as early as 4 to 24 hours after administration of the carcinogen. These changes were nonspecific and consisted of swelling of the cytoplasmic compartments, including the endoplasmic reticulum and nucleolemma. Membrane "whorls" or "fingerprints" were often noted. Autophagic vacuoles were increased in number over those in control animals. Duct cells manifested surface abnormalities, including blebs and "sawtooth" projections (Figure 5).

Table 1—^{3}H-TdR Labeling Index in Pancreatic Acinar Cells After DIPN (in Olive Oil) Administration*

Agent	Weekly DIPN dose (mg/kg body weight)	Number of labeled nuclei/1000 cells† ± SD at											
		1 hr	1 wk	2 wks	5 wks	10 wks	12 wks	15 wks	17 wks	20 wks	22 wks	26 wks	31 wks
DIPN	250	7.38 ±5.84	2.29 2.18	2.08 ±2.20	3.54 ±3.87	3.81 ±3.87	1.46 ±1.24	4.57 ±1.20	5.63 ±2.66	4.79 ±5.73	25.53 ±22.78 (*P* < 0.05)‡	45.74 ±32.97 (*P* < 0.05)‡	47.94 ±35.33 (*P* < 0.05)‡
Olive oil	—	2.48 ± 3.58 (average control value)											

* Hamsters were given weekly subcutaneous injections of DIPN in olive oil. One hour before they were killed, they were given ^{3}H-TdR intraperitoneally (3 μCi/g body weight). Animals (1 to 4/experimental variable) were killed at the time periods shown above.
† Eight hundred to 1200 cells/animal were counted; value listed is mean ± standard deviation.
‡ Calculated by the two-tailed Student's *t* test, when compared to value listed for olive oil (vehicle control).

Table 2—^{3}H-TdR Labeling Index in Pancreatic Acinar Cells After DIPN (in Distilled H_2O) Administration*

Agent	Weekly DIPN dose (mg/kg body weight)	Number of labeled nuclei/1000 cells† ± SD at											
		1 hr	1 wk	2 wks	5 wks	10 wks	12 wks	15 wks	17 wks	20 wks	22 wks	23 wks	26 wks
DIPN	250	1.46 ±1.47	4.37 ±3.49	3.03 ±3.05	2.90 ±1.44	12.22 ±8.68 (*P* < 0.05)‡	22.90 ±15.84 (*P* < 0.05)‡	28.77 ±21.13 (*P* < 0.05)‡	53.47 ±46.50 (*P* < 0.05)‡	26.28 ±11.47 (*P* < 0.05)‡	21.38 ±8.93 (*P* < 0.05)‡	45.93 ±37.25 (*P* < 0.05)‡	12.50§
Distilled H_2O	—	2.41 ± 2.12 (average control value)											

* Hamsters were given weekly subcutaneous injections of DIPN in distilled H_2O. One hour before they were killed, they were given ^{3}H-TdR (3 μCi/g body weight). Animals (1 to 4/experimental variable) were killed at the time periods shown above.
† Eight hundred to 2250 cells/animal were counted; value listed is mean ± standard deviation.
‡ Calculated by the two-tailed Student's *t* test when compared to value listed for distilled H_2O (vehicle control).
§ Due to autolysis only 1 animal received ^{3}H-TdR at the 26 week sacrifice.

Table 3—^{3}H-TdR Labeling Index in Pancreatic Duct Cells After DIPN (in Olive Oil) Administration*

Agent	Weekly DIPN dose (mg/kg body weight)	Number of labeled nuclei/300 cells† ± SD at											
		1 hr	1 wk	2 wks	5 wks	10 wks	12 wks	15 wks	17 wks	20 wks	22 wks	26 wks	31 wks
DIPN	250	1.75 ±2.87	1.00 ±1.41	0.50 ±0.57	0.25 ±0.50	1.84 ±1.71	1.07 ±1.41	2.13 ±2.90	2.68 ±1.99	3.65 ±2.99	6.78 ±4.95 (*P* < 0.05)‡	7.92 ±1.79 (*P* < 0.05)‡	15.00 ±12.73 (*P* < 0.05)‡
Olive oil	—	1.42 ± 2.87 (average control value)											

* Hamsters were given weekly subcutaneous injections of DIPN in olive oil. One hour before they were killed, they were given ^{3}H-TdR intraperitoneally (3 μCi/g body weight). Animals (1 to 4/experimental variable) were killed at the time periods shown above.
† One hundred to 300 cells/animal were counted; value listed is mean ± standard deviation.
‡ Calculated by the two-tailed Student's *t* test, when compared to value listed for olive oil (vehicle control).

Table 4—^{3}H-TdR Labeling Index in Pancreatic Duct Cells After DIPN (in Distilled H_2O) Administration*

Agent	Weekly DIPN dose (mg/kg body weight)	Number of labeled nuclei/300 cells† ± SD at											
		1 hr	1 wk	2 wks	5 wks	10 wks	12 wks	15 wks	17 wks	20 wks	22 wks	23 wks	26 wks
DIPN	250	0.00 ±0.00	0.27 ±0.54	0.95 ±1.12	0.37 ±0.73	6.43 ±5.94 (*P* < 0.05)‡	28.77 ±43.19 (*P* < 0.05)‡	15.83 ±13.91 (*P* < 0.05)‡	11.75 ±13.36 (*P* < 0.05)‡	9.99 ±4.97 (*P* < 0.05)‡	10.14 ±7.68 (*P* < 0.05)‡	10.34 ±9.83 (*P* < 0.05)‡	8.80§
Distilled H_2O	—	0.47 ± 0.80 (average control value)											

* Hamsters were given weekly subcutaneous injections of DIPN in distilled H_2O. One hour before they were killed, they were given ^{3}H-TdR (3 μCi/g body weight). Animals (1 to 4/experimental variable) were killed at the time periods shown above.
† Forty-five to 1100 cells/animal were counted; value listed is mean ± standard deviation.
‡ Calculated by the two-tailed Student's *t* test when compared to value listed for distilled H_2O (vehicle control).
§ Due to autolysis, only 1 animal received ^{3}H-TdR at the 26-week sacrifice.

Table 5—^{3}H-TdR Labeling Index in Pancreatic Islet Cells After DIPN (in Olive Oil) Administration*‡

Agent	Weekly DIPN dose (mg/kg body weight)	Number of labeled nuclei/300 cells† ± SD at											
		1 hr	1 wk	2 wks	5 wks	10 wks	12 wks	15 wks	17 wks	20 wks	22 wks	26 wks	31 wks
DIPN	250	0.25 ±0.50	0.00 ±0.00	0.00 ±0.00	0.50 ±1.00	0.00 ±0.00	0.00 ±0.00	0.67 ±0.71	2.16 ±2.28	0.00 ±0.00	2.78 ±8.19	0.00 ±0.00	0.00 ±0.00
Olive oil	—	1.50 ± 3.30 (average control value)											

* Hamsters were given weekly subcutaneous injections of DIPN in olive oil. One hour before they were killed, they were given ^{3}H-TdR (3 μCi)g body weight). Animals (1 to 4/experimental variable) were killed at the time periods shown above.
† Eighteen to 300 cells/animal were counted; value listed is mean ± standard deviation.
‡ Two-tailed Student's *t* test demonstrated no difference between olive oil (vehicle control) and experimental groups.

Table 6—^{3}H-TdR Labeling Index in Pancreatic Islet Cells After DIPN (in Distilled H_2O) Administration*‡

Agent	Weekly DIPN dose (mg/kg body weight)	Number of labeled nuclei/300 cells† ± SD at										
		1 hr	1 wk	2 wks	5 wks	10 wks	12 wks	15 wks	17 wks	20 wks	22 wks	23 wks	26 wks
DIPN	250	0.88 ±1.02	0.96 ±1.92	0.43 ±0.86	0.00 ±0.00	0.00 ±0.00	0.57 ±0.79	0.31 ±0.54	0.78 ±1.35	0.00 ±0.00	0.20 ±0.41	0.00 ±0.00	0.00
Distilled H_2O	—	0.35 ± 1.10 (average control value)											

* Hamsters were given weekly subcutaneous injections of DIPN in distilled H_2O. One hour before they were killed, they were given ^{3}H-TdR (3 μCi/g body weight). Animals (1 to 4/experimental variable) were killed at the time periods shown above.
† Thirty to 490 cells/animal were counted; value listed is mean ± standard deviation.
‡ Two-tailed Student's *t* test demonstrated no difference between distilled H_2O (vehicle control) and experimental groups.
§ Due to autolysis, only 1 animal received ^{3}H-TdR at the 26-week sacrifice.

In contrast to duct and acinar cells, centroacinar and islet cells were relatively unaffected, but on occasion did manifest similar but more subtle nonspecific ultrastructural alterations.

The first distinctive changes to appear at the light microscopic level were apparent between 1 and 5 experimental weeks. These consisted of acinar cell degeneration (Figure 6) and regeneration, acute ductal inflammation (Figure 7), and hyperplasia (Figure 8). Ultrastructurally (Figures 9 and 10), the duct cells appeared enlarged and increased in number, with irregular luminal surfaces, increased heterochromatin dispersion, and focal cellular necrosis.

In the next stage (5 to 15 weeks), inflammatory changes associated with the ducts disappeared but the ducts remained altered. Acinar cell degeneration and regeneration, however, continued throughout the animals' lifetimes.

In the period between 5 to 15 weeks, multicentric foci of dilated and hyperplastic ducts appeared, often with papillary intraluminal projections (Figures 11–13). These were often grossly visible as minute cysts ($\leq$ 1 mm) throughout the pancreas. When the dilated cystic ducts were contiguous, we termed them *cystic duct complexes* (Figure 12).

Ultrastructurally, these duct complexes were characterized by elongated flattened cells lining dilated structures (Figure 14). The cells comprising the papillary lesions were similar but rested upon well-developed fibrous or fibrovascular stalks.

Cytologically, the epithelial cells comprising the duct complexes showed changes which were mildly atypical, including nuclear enlargement, prominent nucleoli, and irregular chromatin dispersion, but the basal lamina remained intact and there was thus no clear cut evidence of malignancy at this stage.

Chronologically overlapping the appearance of hyperplastic and cystic or papillary cystic duct complexes was the emergence of larger, usually grossly visible ($\geq$ 2 mm), proliferative ductal lesions. These were noted in the time range of 10 to 22 experimental weeks. Because of their histologic complexity, pattern, and size, we termed these lesions *cystadenomas* and *papillary cystadenomas* (Figure 15), rather than hyperplasias, recognizing that these distinctions were somewhat arbitrary. Grossly and microscopically, the hyperplastic duct complexes and the adenomas were similar except that the latter were larger and tended to compress adjacent parenchyma.

In the range of 15 to 23 weeks, we noticed the appearance of distinctly

atypical intraductal lesions (Figures 16–19), with features common to later unequivocal carcinomas. These lesions were characterized by the intraductal proliferation of markedly atypical duct cells, often with complex "bridging" or cribriform patterns, periductal inflammation, and fibrosis.

Ultrastructurally, these intraductal lesions were characterized by the presence of one or more ductal epithelial cell types, including markedly atypical cells with prominent nucleoli located eccentrically and fine chromatin dispersion (Figures 20–21). In these latter cells, the nuclear/cytoplasmic ratio was increased, bizarre nuclear shapes were noted (Figure 20), and the cells appeared rather undifferentiated with respect to cytoplasmic organelles. These atypical and relatively *hypochromatic* (in 1-μ and ultrathin sections) cells could not be distinguished from those seen in unequivocal carcinomas (those which invaded or metastasized), which usually appeared later (17 to 21 weeks). For this reason, we considered these intraductal proliferative lesions to represent carcinoma *in situ*. Indeed, these same lesions were often present in sections alongside invasive ductal carcinomas (Figure 24).

Unequivocal carcinomas were usually found in the 17 to 21 weeks range, although a few appeared as early as 12 weeks in the second experiment. Grossly, they were firm cystic or solid masses, often multiple, readily visible within the pancreas, varying in size from 0.2 to 1.5 cm. They were accompanied by fibrosis, pancreatic atrophy, and adherence to adjacent structures.

At the light microscopic level, these carcinomas consisted of groups of neoplastic ducts replacing large areas of pancreatic parenchyma and were composed of single to multiple layers of neoplastic cells, with surrounding fibrosis and marked chronic inflammation (Figure 22). Evidence of invasion into adjacent structures (Figure 23) or regional node metastasis was often present.

Semithin sections of carcinomas and adjacent pancreatic ducts (Figure 24) revealed a monomorphic cell population—hypochromatic cells with prominent nucleoli.

Ultrastructurally, the tumor cells were usually well-differentiated cells of ductal origin, with very finely dispersed chromatin, except for some clumping just beneath the nuclear envelope. Nucleoli were prominent (Figure 25). The luminal cell surfaces displayed numerous microvilli and surface projections with a well-developed glycocalyx (Figure 26). As expected, contiguous acinar and islet cells manifested varying degrees of degeneration (Figure 27), and disruption of the basal lamina by invading tumor cells was common.

Discussion

In the present study, we have described the morphogenesis of pancreatic adenocarcinoma utilizing the hamster model,[4] which has recently been further refined using a related carcinogen.[9]

We have confirmed the remarkably high incidence of the induced pancreatic neoplasms. Other neoplasms of the gastrointestinal tract as well as the respiratory tract are also encountered in this animal model system [4,10] including hepatic angiosarcomas.

In the original description of this model,[4] pancreatic carcinomas of ductal and acinar cell origin were described. In our study the carcinomas were exclusively of ductal origin. We were able to follow serially the tumor development from early nonspecific ductal changes, followed by duct hyperplasia, and finally to duct adenomas and intraductal and invasive neoplasms. While the various types of lesions tended to be overlapping chronologically, we were nevertheless able to identify a distinctive cell type characteristic of malignant neoplasia.

Both adenomas and carcinomas tended to be multicentric, although occuring less frequently in the area corresponding to the head of the pancreas in the human (where carcinomas are twice as frequent as the body or tail). It is known from numerous serial sections [11] that the hamster pancreas is not entirely similar anatomically to that of the human. The hamster possesses a trilobed organ with confluence of its three main pancreatic ducts and the common bile duct outside the pancreas and duodenum. Hence, the area of pancreas immediately adjacent to the duodenum in the human, which often contains the confluence of the common bile duct and major pancreatic duct, is not found in the hamster. For this reason, we did not see obstructive jaundice in the tumor-bearing animals.

The induced pancreatic neoplasms tended to be distributed distal to the confluence of the pancreatic ducts. Since pancreatic lesions were found as early as 4 to 24 hours after administration of the carcinogen (in acinar cells and intralobular ducts), with progression to larger and larger ducts as a function of time, it is tempting to conclude that the carcinogen (or a metabolic product) reached the parenchymal cells and was then excreted into the duct system. Although bile reflux is physiologically possible in the hamster, this observation does not support the bile reflux theory of pancreatic carcinogenesis.[12]

The effect of inflammation and proliferation of interlobular ducts would obviously have the effect of partial or complete obstruction of ducts distal to these processes and could well lead to dilated or cystic ducts sub-

sequently. Indeed, the cystic duct complexes we observed may be a result of this phenomenon. With the continued administration of carcinogen, these processes would result in a more favorable milieu, by virtue of stasis and obstruction, for repeated insults by the carcinogenic agent, resulting in tumor formation. Thus, a multistage carcinogenic process is entirely consistent with our observations.

Our thymidine incorporation data also tend to support the notion of a multistage process. Although a gradual increase in labeling of duct cells with time is noted, there was, nonetheless, a dramatic multifold increase at 22 weeks (DIPN in olive oil study) and at 10 weeks (DIPN in H_2O study), corresponding precisely to the times when overt neoplasms (adenomas and carcinomas) became histologically apparent, affording a remarkable correlation between the biology and morphogenesis in the hamster model system. The fact that no acinar cell neoplasms developed in our studies would suggest that the concomitant increase in acinar cell labeling was not neoplastic in nature, but rather was regenerative. There is no reason, however, why acinar cell neoplasia might not develop in this system under different experimental conditions. For example, in the original investigation, all but 1 of the animals with acinar cell neoplasms which were dosed in equivalent amounts were females (we employed only male animals in the present study).

Finally, it should be noted that when DIPN is mixed with olive oil, the result is a very poor suspension which leaves large pockets of unabsorbed carcinogen and olive oil in the animals' subcutaneous tissues. When DIPN is mixed with water, a true solution is formed which is readily absorbed from the subcutaneous tissues, affording more uniform dose delivery than with the olive oil. Thus, as might be expected, tumors developed more rapidly and the animals survived a shorter time than when the carcinogen was delivered in olive oil.

References

1. Holland JF, Frei E III (editors): Cancer Medicine. Philadelphia, Lea & Febiger, 1973, p 1559
2. American Cancer Society: Cancer Statistics, 1976. CA 26:22–23, 1976
3. Pledger RA, Bates RR, Saffiotti U: Introduction: National Cancer Institute Pancreatic Carcinogenesis Program. Cancer Res 35:2226–2227, 1975
4. Pour P, Krüger FW, Althoff J, Cardesa A, Mohr U: Cancer of the pancreas induced in the Syrian golden hamster. Am J Pathol 76:349–358, 1974
5. Boren HG, Wright EC, Harris CC: Quantitative light microscopic autoradiography emulsion sensitivity latent image fading. J Histochem Cytochem 12:901–909, 1975
6. Siegel S: Nonparametric Statistics for the Behavioral Sciences. New York, McGraw-Hill Book Co., Inc., 1956, p 152
7. Bloom W, Fawcett DW: A Textbook of Histology, Ninth edition. Philadelphia, W. B. Saunders Co., 1968, pp 97–103, 614–628

8. Althoff J, Pour P, Malick L, Wilson RB: Pancreatic neoplasms induced in Syrian golden hamsters. I. Scanning electron microscopic observations. Am J Pathol 83:517–530, 1976
9. Pour P, Althoff J, Kringer F, Schmahl D, Mohr U: Induction of pancreatic neoplasms by 2,2′-dioxopropyl-*N*-propylnitrosamine. Cancer Letters 1:3–6, 1975
10. Levitt M, Harris C, Squire R, Springer S, Wenk M: Induction of pancreatic neoplasms in Syrian golden hamsters by 2,2′-dihydroxy-di-*N*-propylnitrosamine. Proc Am Assoc Cancer Res 17:41, 1976
11. Pour P: Personal communication
12. Robbins SLR: Pathologic Basis of Disease. Philadelphia, W. B. Saunders Co., 1975, pp 1061–1068

Acknowledgments

The authors greatly appreciate the contributions of Margaret Moore, A.A.S. (Litton-Bionetics, Inc.), and Frank Jackson, Robert Nye, and Maria Yamaguchi for expert technical assistance, and Patricia Hembree (NCI) for excellent secretarial assistance.

Figure 1—Normal hamster pancreatic acinar and centroacinar cells; note pale cytoplasm and paucity of organelles in the latter (× 16,200).

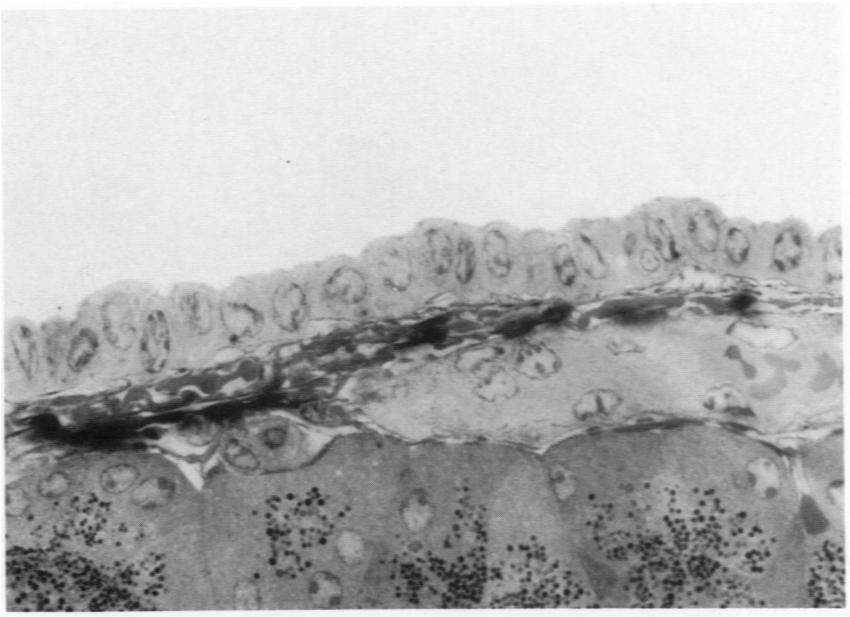

2

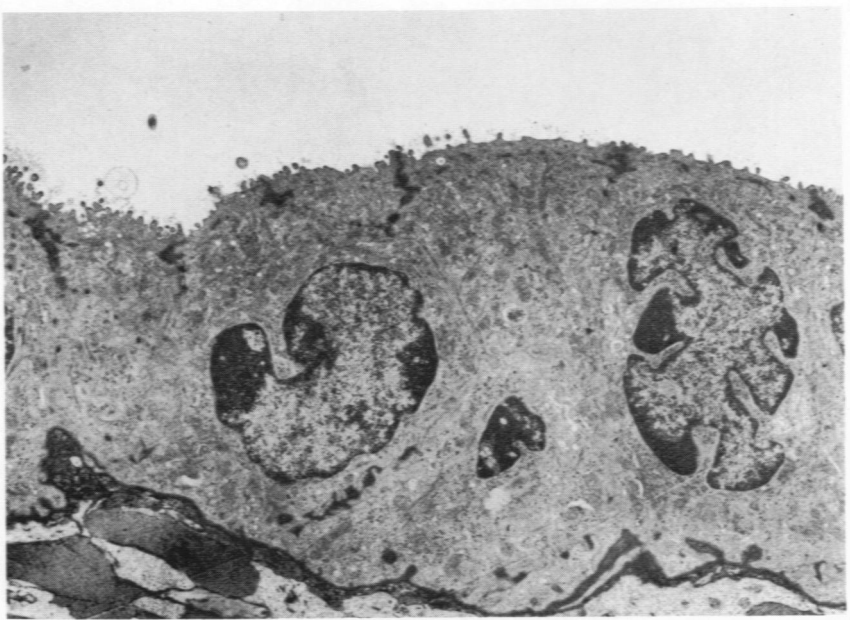

3

Figures 2 and 3—Normal interlobular duct with a single layer of cuboidal to low columnar epithelial cells. Electron micrograph (3) reveals highly convoluted nuclei, prominent peripheral heterochromatin and lack of conspicuous nucleoli. Note irregularly dispersed microvilli. (2, toluidine blue, × 880; 3, × 5250)

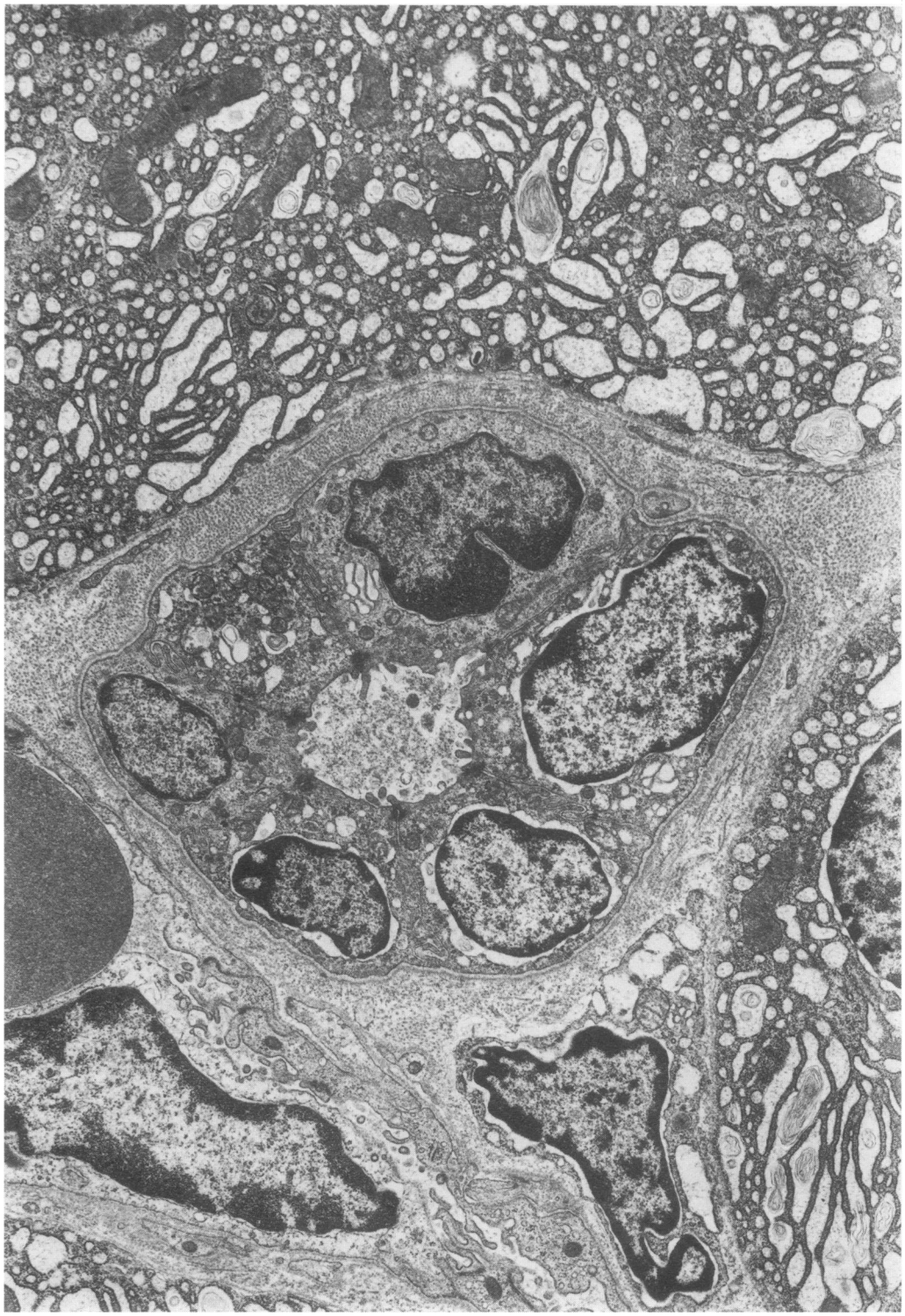

Figure 4—Twenty-four hours after injection of DIPN there is swelling of cytoplasmic compartments in duct and acinar cells and membrane "whorls" within the endoplasmic reticulum of the acinar cells (× 4875).

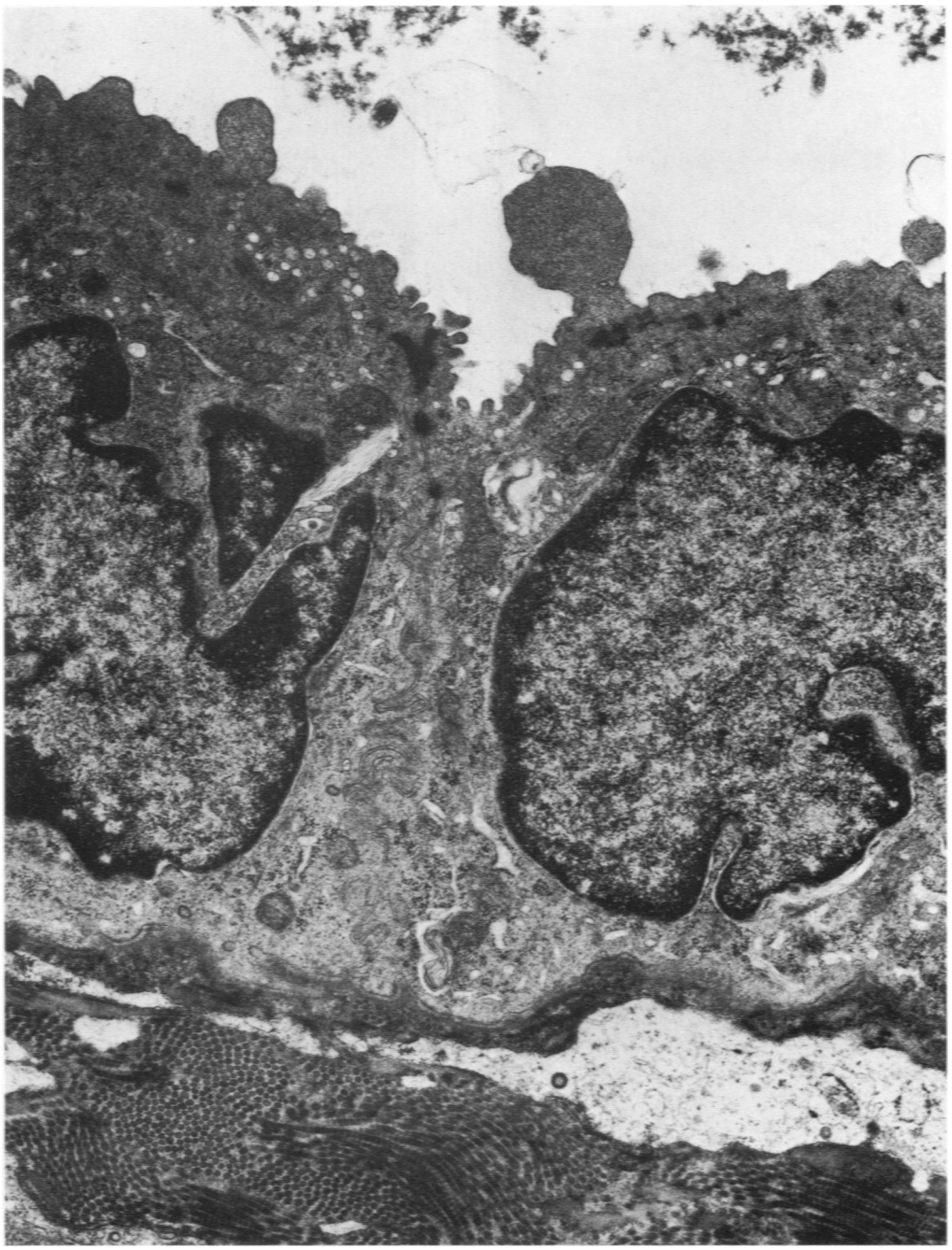

Figure 5—As early as 1 hour after injection of DIPN, duct cells manifest surface irregularities (× 15,000).

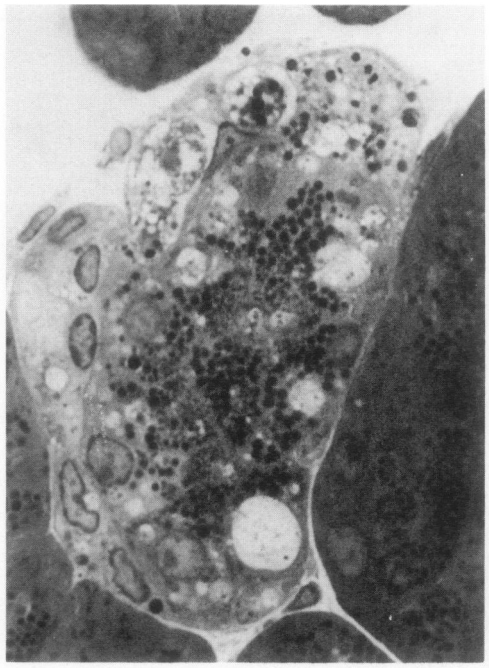

6

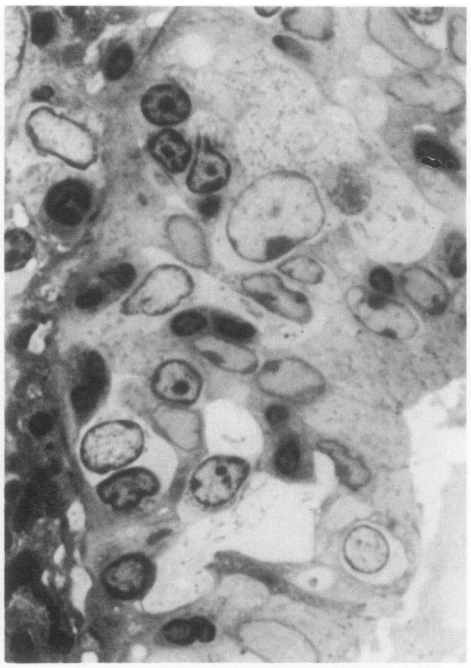

7

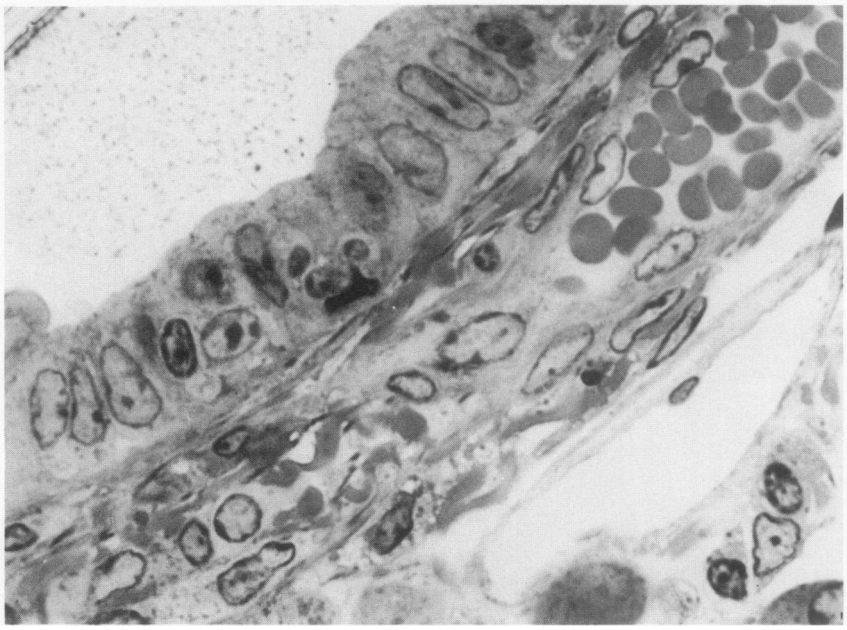

8

Figure 6—Focal lobular degeneration of acinar cells at 5 weeks (Toluidine blue, × 1150). **Figures 7 and 8**—Interlobular ducts at 2 weeks showing acute inflammation, cytolysis, and hyperplasia. Note prominent nucleoli in duct cells. (× 1130)

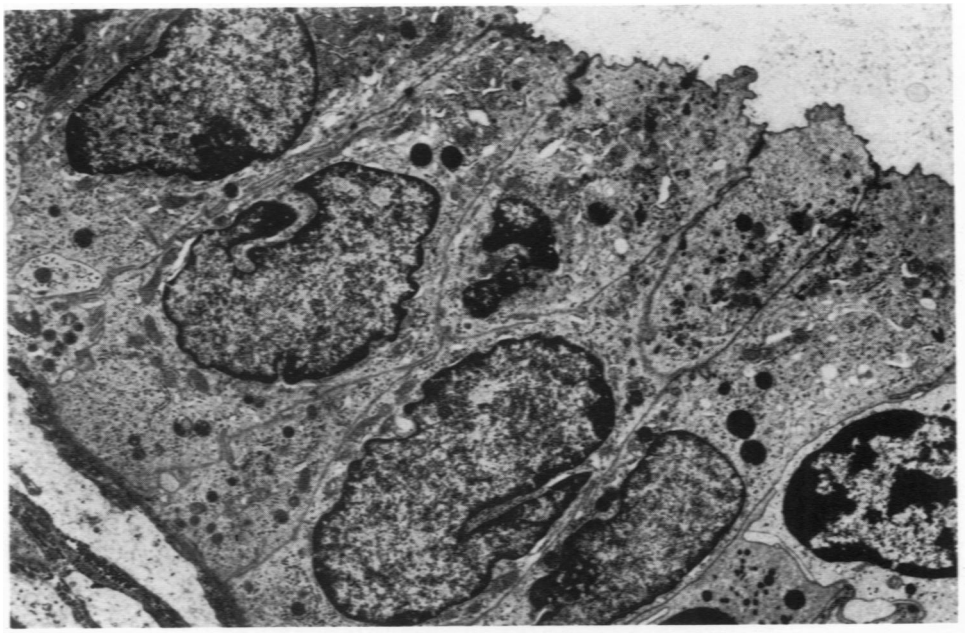

9.

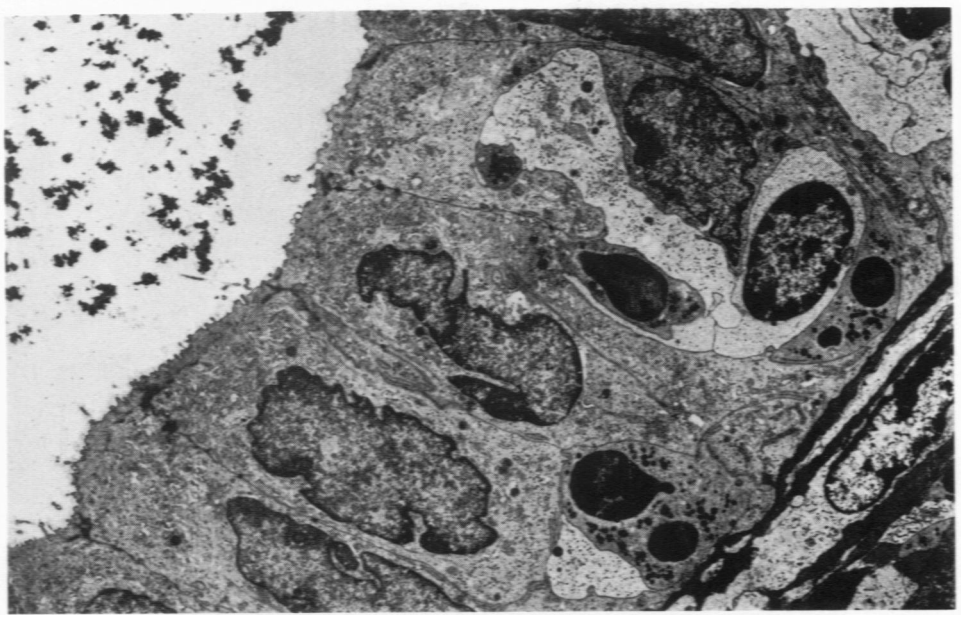

10.

Figures 9 and 10—Electron microscopic appearance of lesion in Figure 8. In comparison to normal (Figure 3), duct cell nuclei exhibit less prominent heterochromatin and luminal cell surfaces are more irregular. (**9**, × 4500; **10**, × 3150)

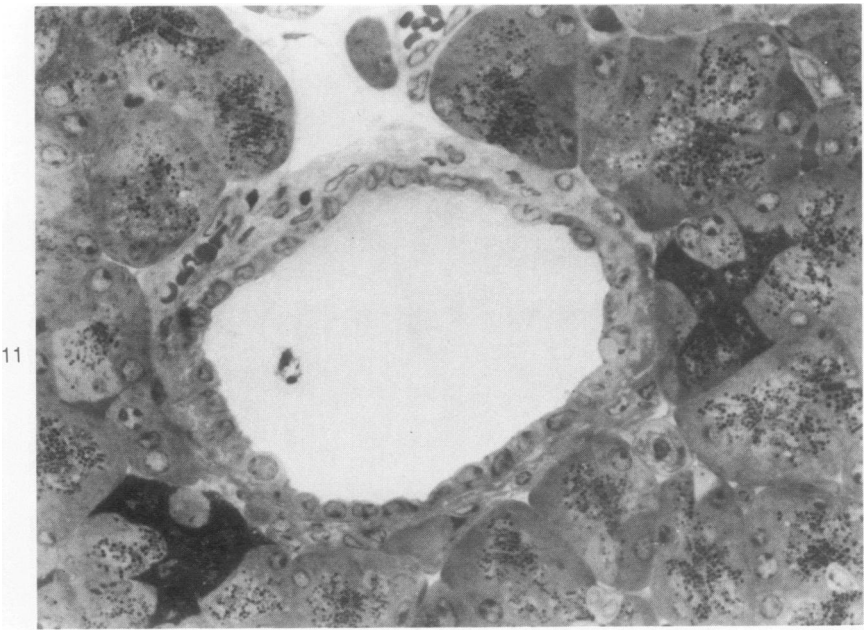

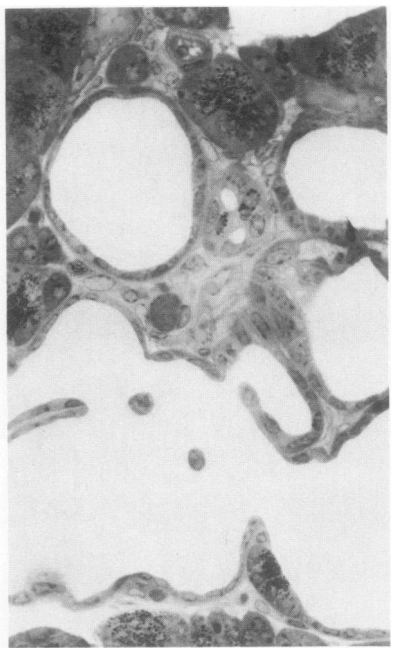

Figure 11—Dilated duct at 10 weeks. Note absence of inflammation at this stage. Dark-staining acinar cells are also seen in untreated animals. (Toluidine blue, × 500) **Figure 12**—Papillary cystic duct complex at 10 weeks (× 350). **Figure 13**—Detail of papillary projection from Figure 12. Note flattened elongated epithelial cells. (× 1130)

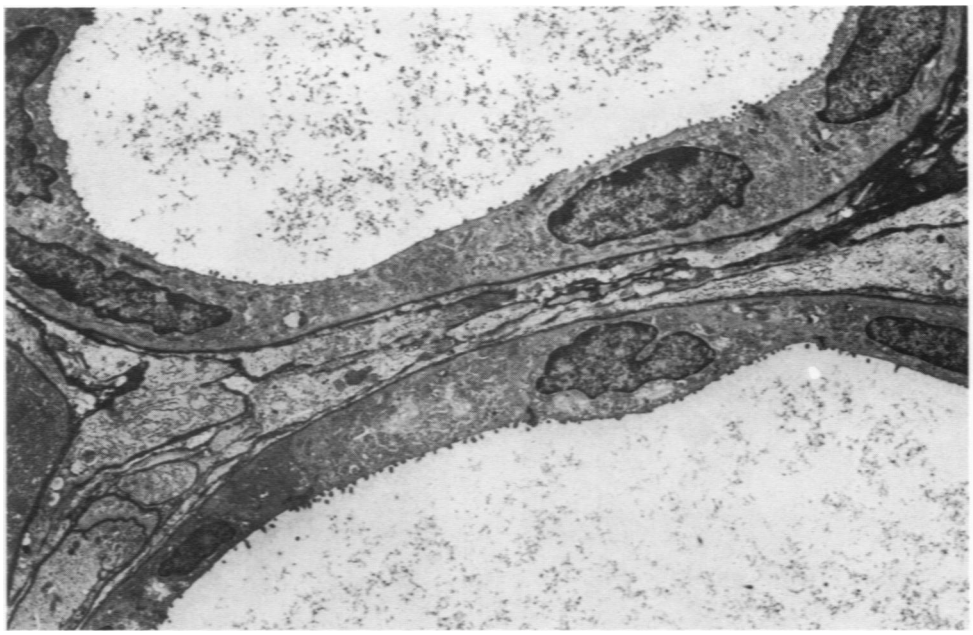

14

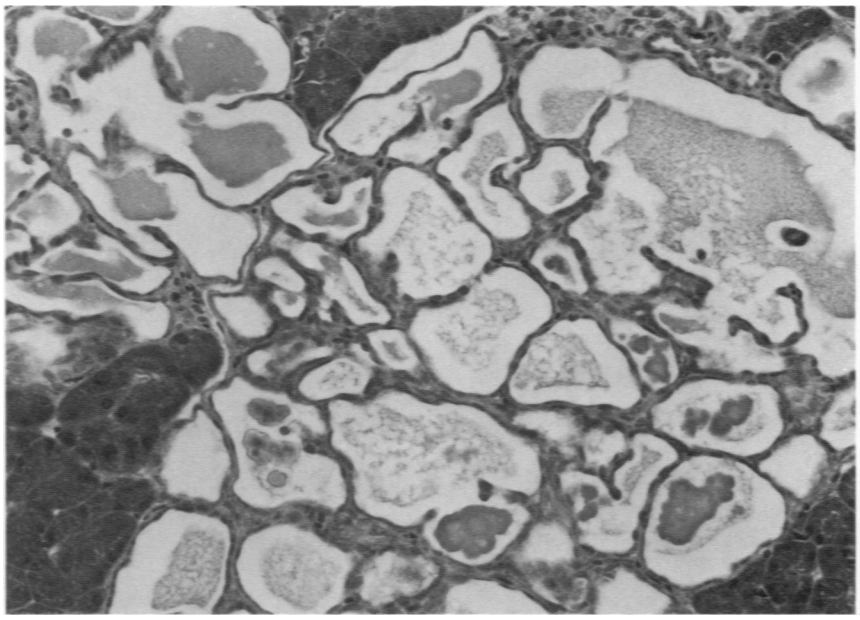

15

Figure 14—Electron microscopic appearance of lesion in Figure 12. Epithelial cells are much flattened and elongated. (× 3000) **Figure 15**—Multilocular ductal cystadenoma at 16 weeks (H&E, × 220).

16

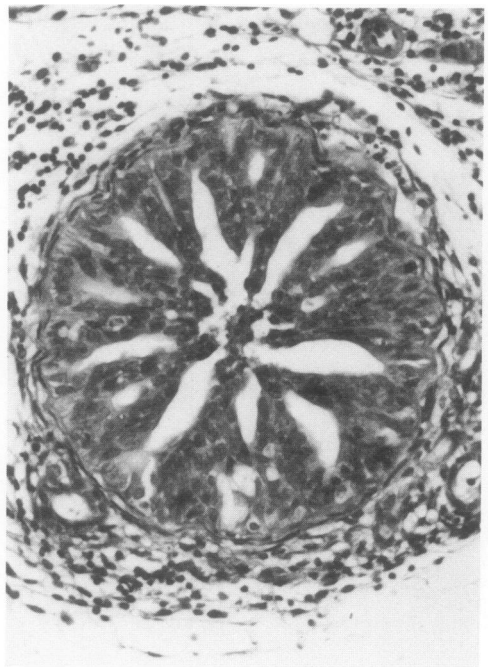

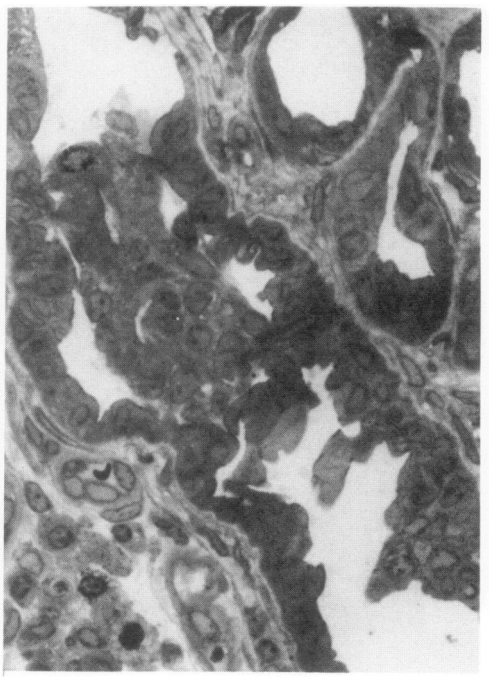

17

18

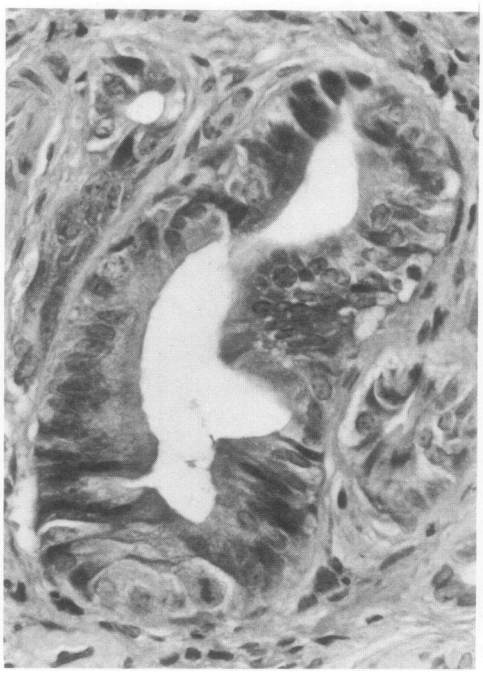

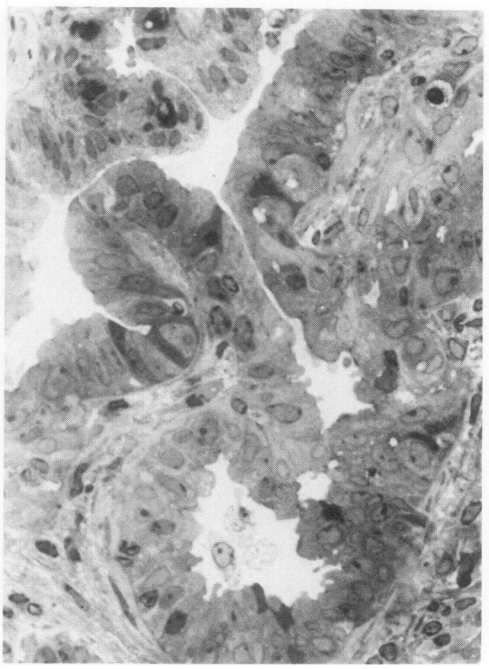

19

Figures 16-19—Marked intraductal proliferation at 15 to 23 weeks, considered to be carcinoma *in situ* (see text). Note complex patterns of epithelial proliferation, periductal inflammation and fibrosis. A mitotic cell is visible in the lower portion of Figure **18.** In the 1-μ sections (Figures **17** and **19**) the duct cells are relatively hypochromatic with prominent nucleoli. (**16,** H&E, × 240; **17,** toluidine blue, × 500; **18,** H&E, × 400; **19,** toluidine blue, × 400).

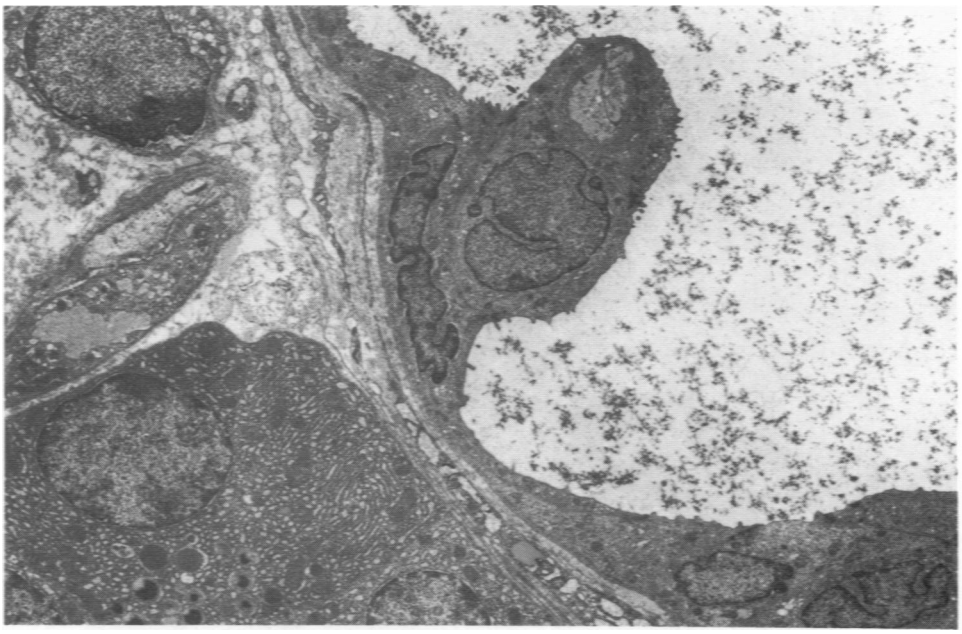

20

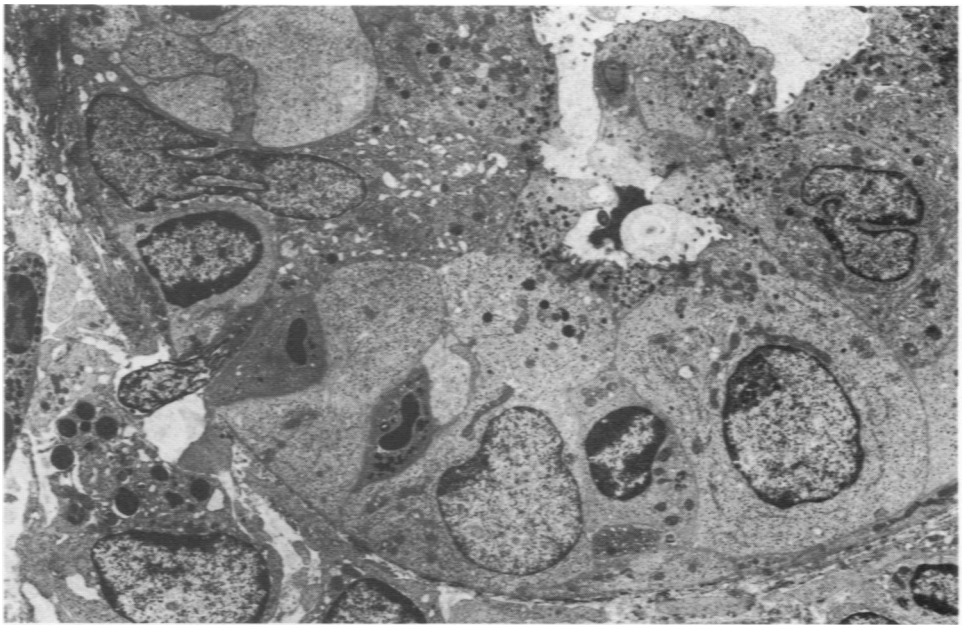

21

Figure 20—Electron microscopic appearance of lesion in Figure 19. Note large atypical cell projecting into lumen with bizarre nuclear membrane features including knob-like extensions. (× 3600) **Figure 21**—Probable intraductal carcinoma at 20 weeks (see text). There is marked inflammation and cytolysis. Note the disruption of the basal lamina at the lower left through which inflammatory cells are migrating. (× 3400)

22

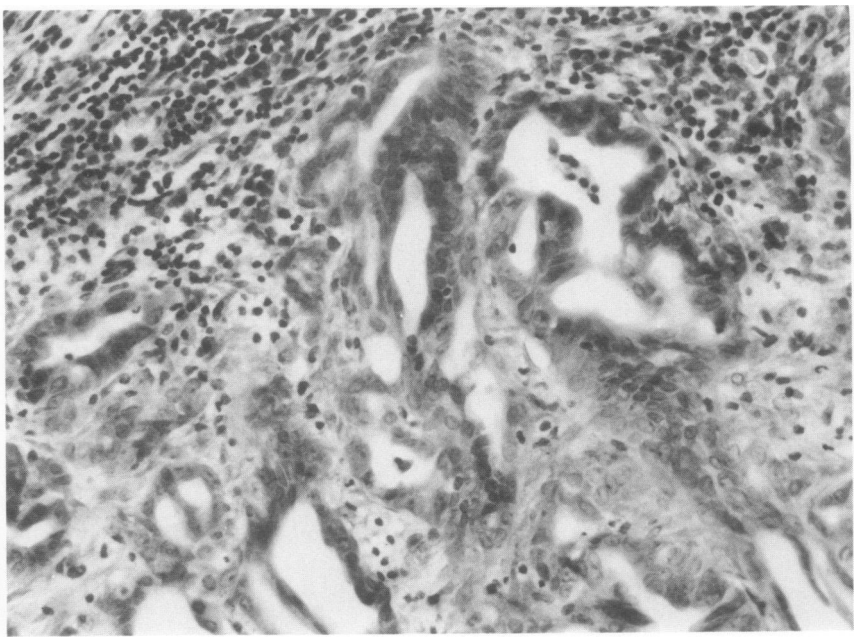

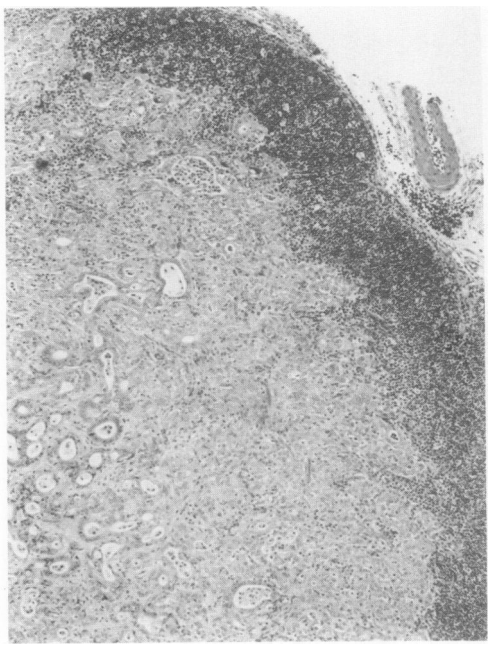

23

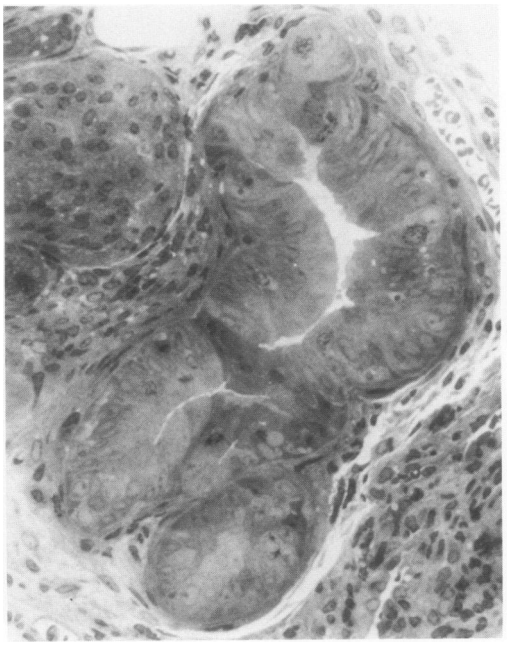

24

Figure 22—Duct carcinoma at 27 weeks eliciting intense inflammatory response (H&E, × 380). **Figure 23**—Duct carcinoma at 31 weeks invading spleen (H&E, × 55). **Figure 24**—Duct from animal with invasive carcinoma at 12 weeks; note characteristic morphology in this 1-μ section (Toluidine blue, × 290).

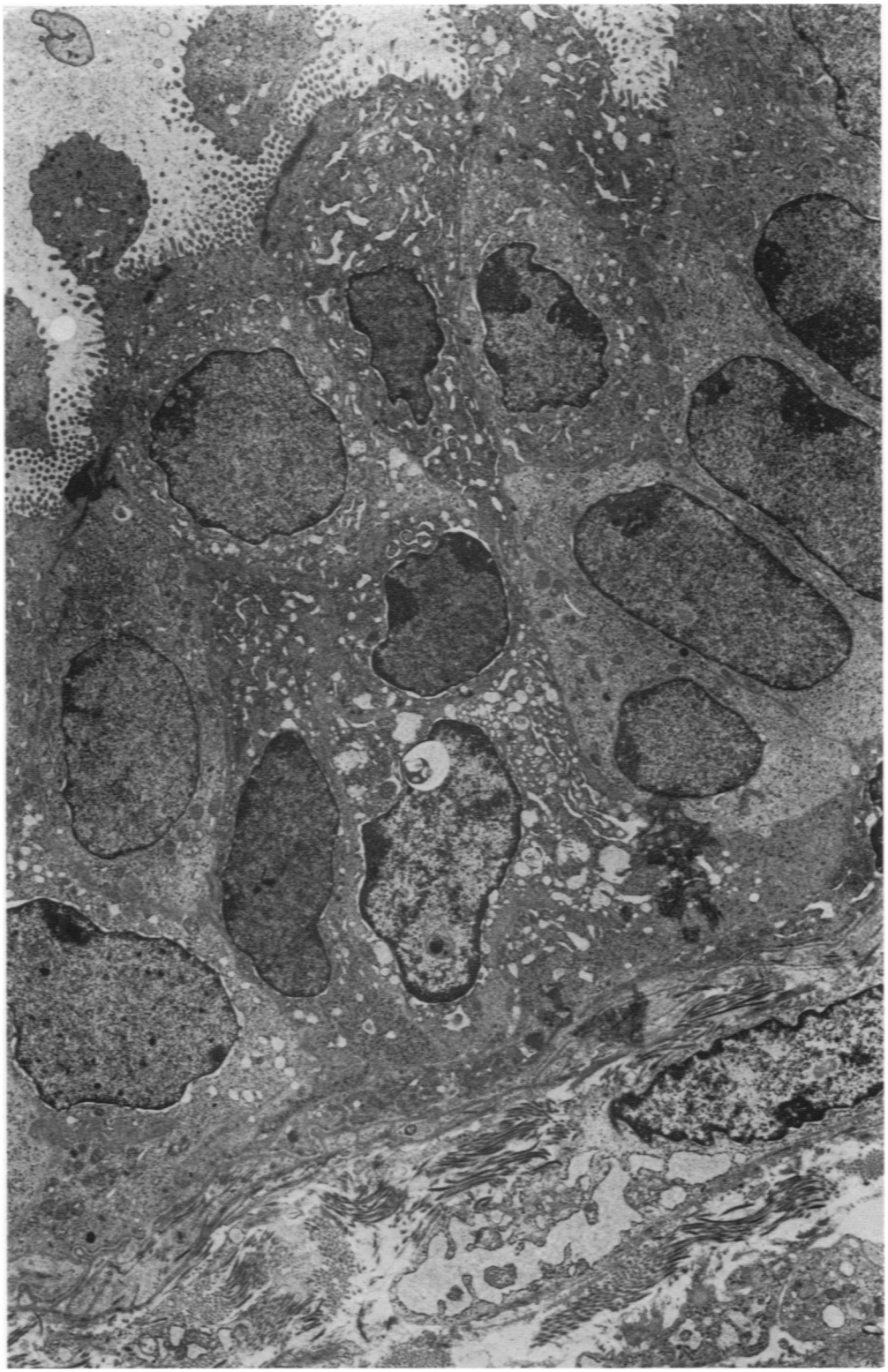

Figure 25—Duct carcinoma at 22 weeks. Typical neoplastic epithelial cell exhibits high nuclear/cytoplasmic ratio, nuclear hypochromasia, very prominent nucleolus, and a marked increase in number of luminal microvilli. (× 5250)

26

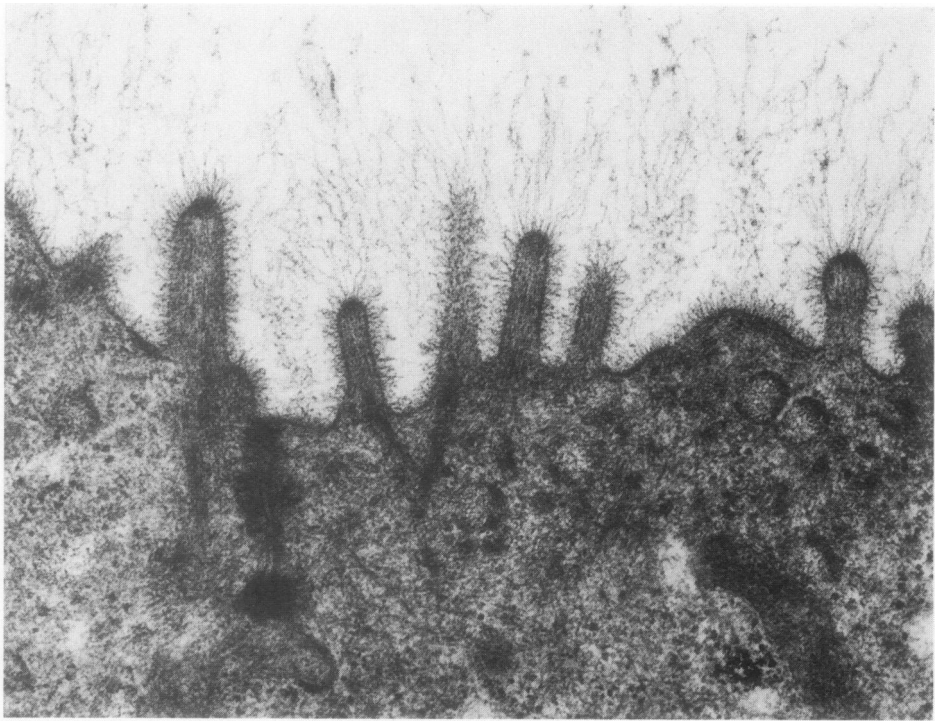

27

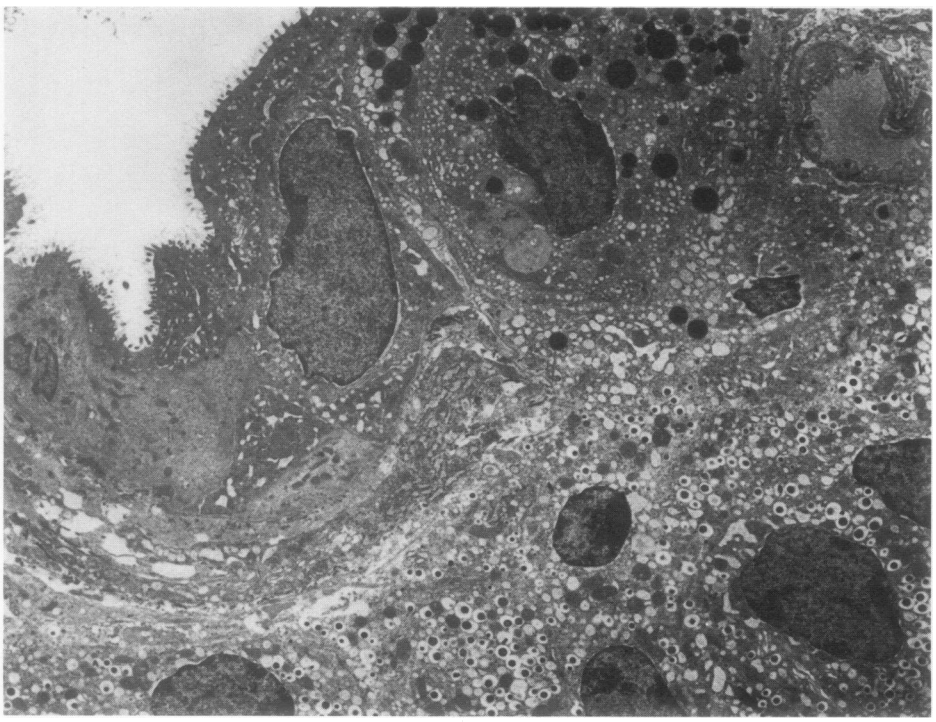

Figure 26—High power detail of luminal membrane of duct carcinoma cells at 17 weeks showing well-developed glycocalyx (× 36,000). **Figure 27**—Duct carcinoma at 17 weeks. Note degenerating acinar (*upper right*) and islet (*lower right*) cells adjacent to neoplastic duct at left. (× 3150)